Available online at www.sciencedirect.com
SCIENCE DIRECT
Trans. Nonferrous Met. Soc. China 16(2006) 992−997
Transactions of Nonferrous Metals Society of China
www.csu.edu.cn/ysxb/

Effect of oxygen impurity on long-term thermal stability of Zr-based metallic glasses below glass transition temperature

HE Lin (贺 林)[1], ZHANG Shuai(张 帅)[1], SUN Jun(孙 军)[1], ZHANG Chang-jun(张长军)[2]

1. State Key Laboratory for Mechanical Behavior of Materials, Xi'an Jiaotong University, Xi'an 710049, China;
2. Construction Machinery School, Chang'an University, Xi'an 710049, China

Received 16 November 2005; accepted 29 April 2006

Abstract: Long-term thermal stability of a series of Zr-based metallic glasses with different oxygen contents below their glass transition temperatures was compared based on their deductive continuous-heating-transformation diagrams created by using the corollary of Kissinger analysis method. It is found that the influence of oxygen on the long-term thermal stability of Zr-based metallic glasses exhibits at lower temperature is different from that on their short-term thermal stability presented at higher temperature. For each kind of the Zr-based metallic glasses, there is a critical heating rate, ϕ_c, which corresponds to a critical temperature, T_c. As heating rate is smaller than ϕ_c and onset devitrification temperature is below T_c, the glass with higher oxygen content will have longer incubation period for onset devitrification. The values of ϕ_c and T_c are related with the glasses' reduced glass transition temperature T_{rg}. The improving effect of oxygen impurity on the long-term thermal stability of Zr-based metallic glasses was discovered.

Keywords: Zr-based metallic glasses; thermal stability; continuous heating transformation diagram; oxygen impurity

1 Introduction

Metallic glasses as disordered solids are thermodynamically metastable at the temperature below their glass transition temperatures, T_g. Phase transformation of devitrification being activated by time and temperature can occur not only above T_g with shorter incubation period but also below T_g with longer incubation period[1]. The long-term thermal stability of metallic glasses below their T_g is one of the most important properties influencing their engineering applications[2]. Supercooled liquid region ΔT_X(=T_X−T_g, T_X is the onset devitrification temperature above T_g at a certain heating rate) usually is employed as the parameter to characterize the short-term thermal stability of metallic glasses at temperature above T_g[3]. Time—temperature—transformation(TTT) diagrams created in isothermal mode are useful for the evaluation of full—scale—term thermal stability of metallic glasses. However, the long-term scale parts of TTT diagrams require long-term annealing to be constructed. Continuous—heating—transformation(CHT) diagrams under continuous heating mode can be created by using the corollary of the Kissinger analysis method and the long-term thermal stability of metallic glasses can be evaluated according to the long-term scale parts of the deductive CHT diagrams [2].

Zr-based metallic glassy alloys have high glass-forming ability (GFA) and good short-term thermal stability characterized by large ΔT_X, excellent strength and better corrosion resistance, which enable them for use in engineering applications as structural metallic materials[4,5]. The effect of oxygen impurity on the GFA and short-term thermal stability of Zr-based metallic glassy alloys has already been studied in detail by several different groups over the years[6, 7]. It is clear that even a small quantity of oxygen impurity in Zr-based metallic glasses is detrimental to their GFA and short-term thermal stability. However, the influence of oxygen impurity on the long-term thermal stability of Zr-based metallic glasses below their glass transition temperatures has been rarely considered, though which is important for their engineering applications. Certain level of oxygen in the glasses coming from raw materials or atmosphere is expected and unavoidable under ordinary laboratory and industrial processing conditions because of the strong affinity of zirconium with oxygen[8].

Formation item: Project(50671076) supported by the National Natural Science Foundation of China
Corresponding author: HE Lin; Tel: +86-29-82665165; E-mail: helin@mail.xjtu.edu.cn

Demanding limit to the oxygen content will make the manufacture cost of Zr-based metallic glasses very high. Thereby the influence of oxygen impurity on the long-term thermal stability of Zr-based metallic glasses is worthy of investigation. In this paper the long-term thermal stability of a series of Zr-based metallic glasses with different oxygen contents is compared based on their deductive CHT diagrams.

2 Experimental

2.1 Preparation of Zr-based metallic glasses

Ternary alloy $Zr_{50}Cu_{40}Al_{10}$, quaternary alloy $Zr_{65}Cu_{17.5}Ni_{10}Al_{7.5}$ and quinary alloy $Zr_{52.5}Cu_{17.9}Ni_{14.6}Al_{10}Ti_5$ were chosen as the base alloys in current study. High-purity crystal Zr (99.9%, mass fraction) containing about 7.0×10^{-4} O (molar fraction) was used for preparation of the specimens with lower oxygen content. Low-purity sponge Zr (97.72% Zr+1.68% Hf, mass fraction) containing about 5.0×10^{-3} O (molar fraction) was used as the partial substitute of crystal Zr for preparation of the specimens with higher oxygen content. INOUE et al[9] found that a small amount of Hf in Zr-based BMGs has no notable effect on their GFA and thermal stability, so the use of sponge Zr in current study mainly increases the oxygen impurity content in the alloys. Cu, Ni, Al and Ti used have purities of 99.9 % (mass fraction).

The wedge-like specimen with a width of 25 mm, a length of 75 mm and a varying thickness from 1.5 mm to 12 mm along the length axis was prepared for each kind of alloy by tilt casting method using a ladle hearth type arc furnace[10]. As shown in Fig.1, the master alloy was melted under a Ti-gettered argon atmosphere and then cast into a copper mold by tilting the hearth. Alloy liquid flowed freely into the mold's chamber just under the action of gravity in this method. To eliminate the 'crystal-nuclei' on the bottom of copper hearth and obtain a homogeneous alloy melt, master alloy was completely remelted more than four times and electromagnetically stirred during the whole melting process. Oxygen concentration of the specimens prepared was measured by hot extraction using a LECO RO-416D2 analyzer. Analysis indicates that the three kinds of alloys made of high-purity crystal Zr contain $(6.0-7.0)\times10^{-4}$ O (molar fraction), which are designated as Specimen TE-1, QU-1 and QI-1. The alloys with partial substitute of the low-purity sponge Zr contain $(2.0-2.3)\times10^{-3}$ O (molar fraction), which are designated as Specimen TE-2, QU-2 and QU-2. The specimens' codes and their detailed oxygen contents are listed in Table 1.

The wedge-like specimens prepared were cut into slices of 3 mm in thickness perpendicularly to the length axis. These pieces were analysed by X-ray diffracometry (XRD) using a D/MAX 2400 diffractometer with Cu K_α radiation. The maximum thickness does not show any detectable crystal peak on the XRD pattern, which represents the maximum glass-forming thickness of each alloy, t_{max}, was determined. Differential scanning calorimetry(DSC) was performed using a SETARAM Labsys^{TM} TG DSC in an argon atmosphere with the heating rates of 0.083, 0.17, 0.33 and 0.67 K/s and sample mass of (30 ± 1) mg.

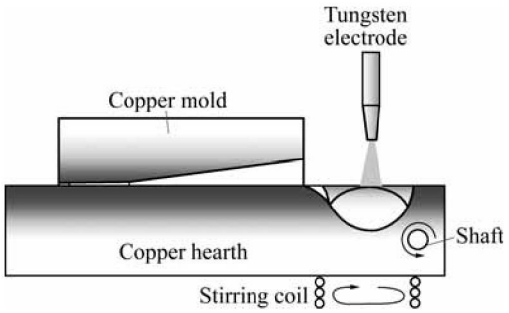

Fig.1 Schematic illustration of tilt casting method

2.2 Construction of CHT diagrams

The Kissinger equation describes the rate of a transformation process as [11]

$$\frac{dx}{dt}=A(1-x)^{n'}\exp(-E/RT) \quad (1)$$

where x is volume fraction transformed, t is time, n' is the transformation order, A is a constant and R is the gas constant. Based on Eqn.(1), the Kissinger plot for continuous heating mode can be derived

Table 1 Specimen codes, compositions, t_{max}, specific temperature at 0.67 K/s heating rate and activation energy of Zr-based metallic glasses

Code	Base composition	x(O)/10^{-4}	t_{max}/mm	T_g / K	T_X / K[1)]	ΔT_X / K	E_X/(kJ·mol^{-1})
TE-1	$Zr_{50}Cu_{40}Al_{10}$	6.76	5.1	697.7	784.9	87.2	384.6
TE-2	$Zr_{50}Cu_{40}Al_{10}$	22.67	3.5	705.9	773.7	67.8	431.8
QU-1	$Zr_{65}Cu_{17.5}Ni_{10}Al_{7.5}$	5.95	4.2	638.5	747.2	108.7	271.8
QU-2	$Zr_{65}Cu_{17.5}Ni_{10}Al_{7.5}$	21.15	1.8	642.6	740.0	97.4	296.1
QI-1	$Zr_{52.5}Cu_{17.9}Ni_{14.6}Al_{10}Ti_5$	6.84	6.5	675.5	731.2	55.7	325.5
QI-2	$Zr_{52.5}Cu_{17.9}Ni_{14.6}Al_{10}Ti_5$	19.82	4.5	676.3	738.8	62.5	364.8

1) Onset pre-devitrification temperture for quinary alloy.

$$\ln(\frac{\phi}{T_p^2}) = -\frac{E}{RT_p} + c \tag{2}$$

where ϕ is the heating rate, i.e., dT/dt. T_p is the peak temperature at which the transformation rate dx/dt attains the maximum value, c is a constant. Eqn.(2) can be used for determination of the kinetic constants of transformations studied using differential thermal analysis(DTA) or differential scanning calorimetry(DSC) under continuous heating mode. Although the Kissinger plot has been widely applied to the devitrification of a large number of metallic glasses, it should be mentioned that Eqn.(2) is based on Kissinger equation. In fact, the devitrification of metallic glasses can be well described by the isothermal Johnson-Mehl-Avrami equation as[12]

$$x = 1 - \exp\left\{-\left[k_T(t-\tau)\right]^n\right\} \tag{3}$$

where τ corresponds to a time lag or incubation time, n is the Avrami exponent and k_T is the reaction rate constant which is related to the activation energy, E, and the frequency factor, ν, through the Arrhenius temperature dependence[13]:

$$k_T = \nu \exp\left(-\frac{E}{RT}\right) \tag{4}$$

By taking the first derivative of Eqn.(3), the rate of the devitrification can be expressed as

$$\frac{\mathrm{d}x}{\mathrm{d}t} = k_T n(1-x)\left(\ln\frac{1}{1-x}\right)^{(n-1)/n} \tag{5}$$

Based on Eqns.(5) and (4), CHEN[14] derived the following formula to the continuous heating devitrification of metallic glasses by considering the fact $E/RT \gg 1$:

$$\ln(\frac{\theta^2}{\phi}) = \frac{E}{R\theta} + c \tag{6}$$

where θ is the specific temperature corresponding to any certain crystalline volume fraction transformed during a continuous heating process. It is clear that Eqn.(6) is the same as Eqn.(3) if $\theta = T_p$, so it is the general form of the Kissinger plot. Eqn.(6) can be used to any certain devitrification degree, e.g. onset, peak or completion devitrification. The plot of $\ln(\theta^2/\phi)$ vs $1/\theta$ yields a straight line and the slope is related to the activation energy corresponding to the selected devitrification degree.

During a DSC or DTA run from room temperature (supposed 298 K) with a constant heating rate, ϕ, the specific temperature, θ, is related to the heating time, t_θ, by $\theta = \phi t_\theta + 298$. Thus Eqn.(6) can be rewritten as

$$t_\theta = \frac{\theta - 298}{\theta^2}\exp\left(\frac{E}{R\theta} + c\right) \tag{7}$$

The relationship between t_θ and θ can be determined after the tangent (E/R) and intercept (c) constants of the Kissinger plot of specific temperature θ are obtained.

3 Results and discussion

The maximum glass-forming thicknesses of the three kinds of alloys with lower and higher oxygen contents based on XRD analysis is list in Table 1. It is doubtless that oxygen impurity makes the GFA of the Zr-based metallic glasses, especially that of the quaternary alloy seriously decreases, which is consistent with the former research results in Refs.[15−17].

Fig.2 shows the DSC curves of the three kinds of glasses with lower and higher oxygen contents. All the samples for DSC test were taken from the glassy part of each wedge-like specimen. It can be seen from Fig.2 that the DSC curves of the ternary and quaternary alloys keep their single peak characteristic at different heating rates in the oxygen content range investigated (Specimen TE-1 and TE-2, QU-1 and QU-2), however, the specific

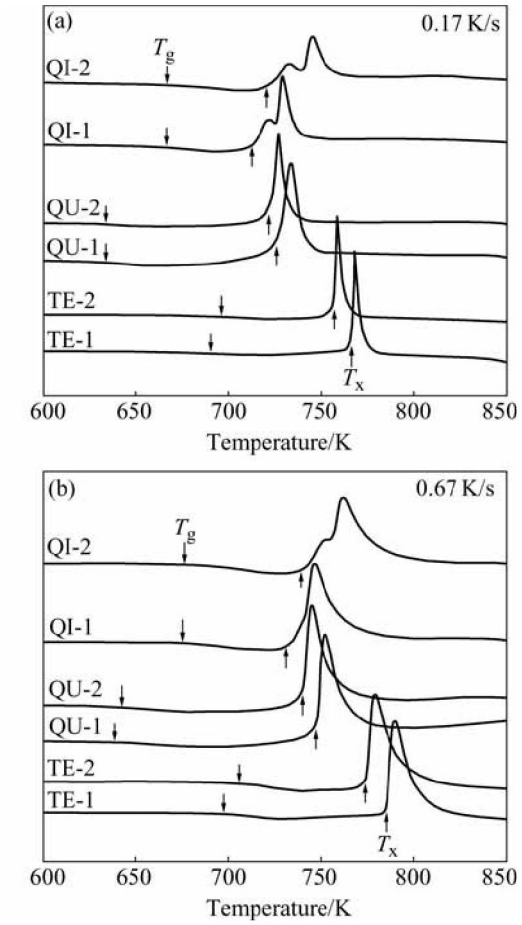

Fig.2 DSC curves of Zr-based metallic glasses with different oxygen contents at heating rates of 0.17 K/s(a) and 0.67 K/s(b)

temperatures T_X, T_p (peak temperature of devitrification) and ΔT_X of the specimens with higher oxygen contents (Specimen TE-2 and QU-2) clearly decline, which means that the short-term thermal stability of these two kinds of glasses is lowered by oxygen impurity. The quinary alloy has the DSC curve composed of a pre-devitrification peak (lower in intensity) at lower temperature and a main-devitrification peak (higher in intensity) at higher temperature (Specimen QI-1 and QI-2), the two peaks tend toward partially overlapping as the heating rate increases. Oxygen in the content range investigated does not evidently influence the basic form of the DSC curves at different heating rates, however, the specific temperatures T_X (onset pre-devitrification temperature), T_P (peak temperature of main-devitrification) and ΔT_X of the specimen with higher oxygen content (Specimen QI-2) evidently rises, which means the short-term thermal stability of the quinary glass is enhanced by oxygen impurity. For the purpose of comparison, the specific temperatures of the three kinds of alloys with lower and higher oxygen contents at 0.67 K/s heating rate are listed in Table 1.

Fig.3 shows the Kissinger plots of T_X for the three kinds of metallic glasses. It can be seen that all the plots have good linear relationships. The activation energy of onset devitrification, E_X, estimated from the slopes of the Kissinger plots of T_X are also listed in Table 1. It is interesting to note that the E_X of each kind of the alloys are obviously increased with the increase of oxygen contents, which is not consistent with their changing tendencies of the GFA characterized by t_{max}. This inconsistency has also been discovered elsewhere for other BMGs[18,19]. The reason should be that the GFA of metallic glasses is simultaneously influenced by their thermodynamic and kinetic factors not only by their activation energy, so the inconsistency could be understood.

Applying the tangent (E_X/R) and intercept (c)

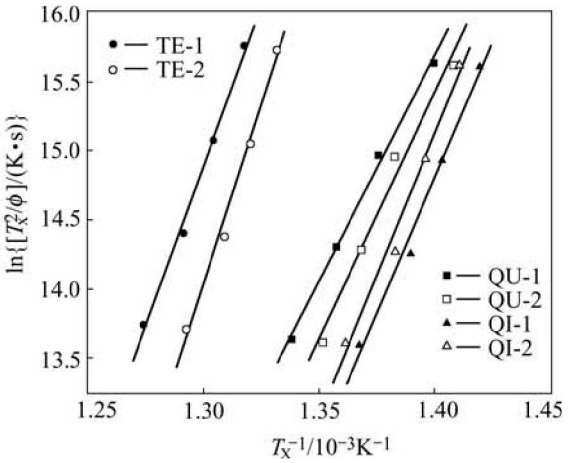

Fig.3 Kissinger plots of T_X for Zr-based metallic glasses with different oxygen contents

constants of the Kissinger plots of T_X in Fig.3 to Eqn.(7), T_X vs t_X plots corresponding to onset devitrification for different specimens can be created as shown in Fig.4. It can be seen from Fig.4 that the average temperature slope of the onset devitrification CHT curve for each kind of the alloys is changed by oxygen impurity. The curves of the specimens with higher oxygen contents (Specimen TE-2, QU-2 and QI-2) have lower average temperature slope. For each kind of the alloys, there is a

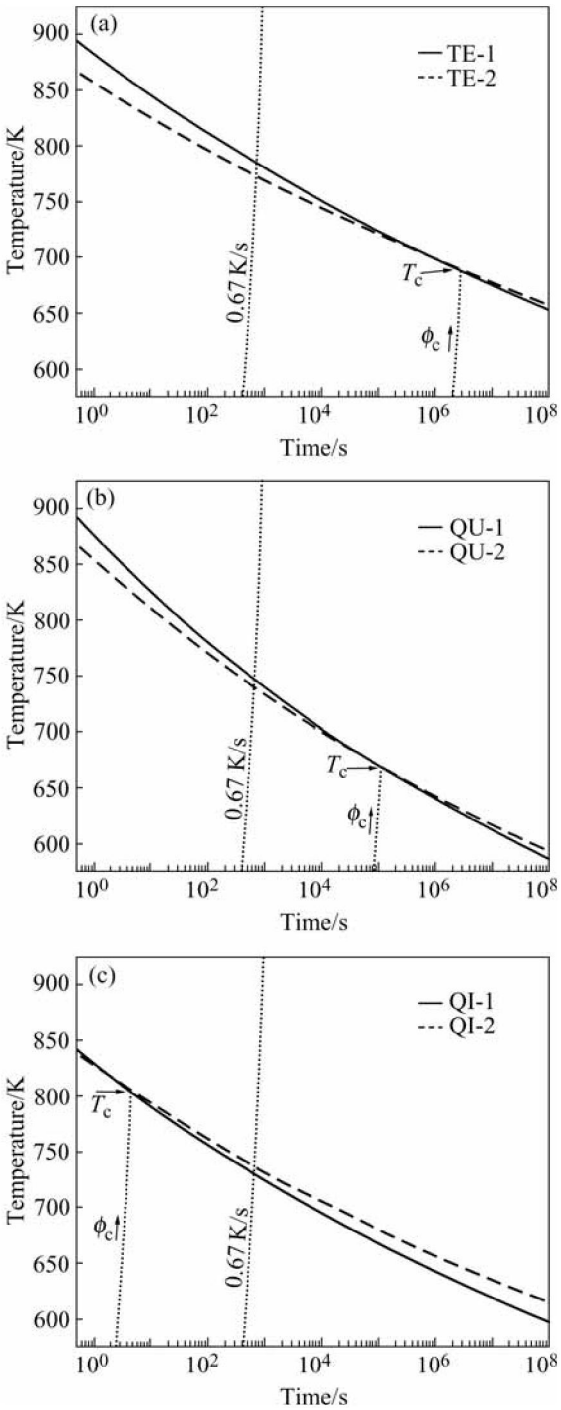

Fig.4 Deductive CHT diagrams of ternary (a), quaternary (b) and quinary (c) Zr-based metallic glasses with different oxygen contents corresponding to T_X

critical heating rate, ϕ_c, which corresponds to a critical temperature, T_c. If onset devitrification temperature is above T_c as heating rate is larger than ϕ_c, the specimen with higher oxygen content will have shorter incubation period for onset devitrification. On the contrary, if onset devitrification temperature is below T_c as heating rate is smaller than ϕ_c, the specimen with higher oxygen content will have longer incubation period for onset devitrification. Thus it can be concluded that the influence of oxygen on the long-term thermal stability of Zr-based metallic glasses at lower temperature is different from that on their short-term thermal stability presented at higher temperature. Although oxygen impurity decreases the short-term thermal stability of Zr-based metallic glasses, which is closely correlative with their reduced GFA, their long-term thermal stability is enhanced at the same time.

CHEN et al[20] studied the oxygen dissolution in a Zr-based metallic glass and oxygen redistribution during its nanodevitrification using three dimensional atom probe (3DAP). It is found that oxygen distribution in the initial supercooled liquid is uniform, the first step for oxygen to promote the nucleation of crystal phase(s) is its redistribution by atom diffusion. It is well know that the speed of atom diffusion in a supercooled liquid depends to a great extent on its viscosity, $\eta(T)$. The temperature dependence of $\eta(T)$ can be described by the widely accepted Vogel-Fulcher exponential expression as [21]

$$\eta(T) = A\exp\left(\frac{B}{T - T_0}\right) \tag{8}$$

where A, B and T_0 are constants. The viscosity of a supercooled liquid exponentially increases from 10^{-3} Pa·s to 10^{12} Pa·s during the cooling process from T_l (liquidus temperature) to T_g[21]. Oxygen redistribution occurs faster in the supercooled liquid with lower viscosity at higher temperature, which can increase the crystal nucleation tendency of Zr-based metallic glasses and thereby decreases their GFA and short-scale thermal stability. On the contrary, the rapid increase of the viscosity of supercooled liquid at lower temperature can limit oxygen redistribution, which can alleviate or eliminate its detrimental effect. Moreover, KÜBLER et al[22] found that oxygen also had the effect of remarkable increasing the viscosity of Zr-based metallic glass in supercooled liquid region. Synthetically, oxygen in Zr-based metallic glasses enhances the long-scale thermal stability at lower temperature.

The temperature dependence of viscosity, $\eta(T)$, of metallic glasses is also affected by their reduced glass transition temperature, $T_{rg}(=T_g/T_l)$. The larger the T_{rg} is, the rapider $\eta(T)$ increases exponentially with decreasing temperature. After measuring the T_l of the three kinds of Zr-based metallic alloys at the same slow cooling rate of 0.017 K/s, their T_{rg} can be calculated as listed in Table 2. The quinary alloy has the highest T_{rg}, therefore the highest critical temperature, T_c, and the highest corresponding critical heating rate, ϕ_c (Table 2), which makes the quinary alloy with higher oxygen content have better thermal stability at higher temperature. The testing heating rate of 0.67 K/s is larger than the ϕ_c of the ternary and quaternary alloys, therefore the ΔT_X values of Specimens TE-2 and QU-2 are smaller than Specimens TE-1 and QU-1 at this heating rate. However, the testing heating rate of 0.67 K/s is smaller than the ϕ_c of the quinary alloy, so the ΔT_X value of Specimen QI-2 is larger than Specimen QI-1 at the same heating rate.

Table 2 Critical heating rates and corresponding critical temperatures of Zr-based metallic glasses

Code	ϕ_c/(K·s^{-1})	T_c/K	T_l/K	T_{rg}/K
TE	1.4×10^{-4}	689	1 128	0.62
QU	3.2×10^{-3}	669	1 123	0.57
QI	50	805	1 055	0.64

4 Conclusions

Long-term thermal stability of the Zr-based metallic glasses with different oxygen impurity contents can be compared based on their deductive CHT diagrams created by using the corollary of the Kissinger analysis method. Oxygen impurity has the tendency to make the activation energy for onset devitrification of $Zr_{50}Cu_{40}Al_{10}$, $Zr_{65}Cu_{17.5}Ni_{10}Al_{7.5}$ and $Zr_{52.5}Cu_{17.9}Ni_{14.6}Al_{10}Ti_5$ metallic glasses increase. As a result, the influence of oxygen on the long-term thermal stability of the Zr-based metallic glasses exhibiting at lower temperature is different from that on their short-term thermal stability presented at higher temperature. Although oxygen impurity decreases the glasses' GFA characterized by t_{max} and short-term thermal stability characterized by ΔT_X, their long-term thermal stability is enhanced at the same time. Oxygen impurity has the positive effect on the long-term thermal stability of Zr-based metallic glasses below their glass transition temperatures. Appropriate permission of certain oxygen impurity content in the designing of Zr-based metallic glasses for engineering applications will not only decrease their high manufacture cost, but also increase their long-scale thermal stability.

References

[1] LUBORSKY F E. Amorphous Metallic Alloys [M]. London: Butterworths, 1989: 144−168.

[2] LOUZGUINE D V, INOUE A. Comparison of the long-term thermal stability of various metallic glasses under continuous heating [J]. Scripta Mater, 2002, 47(12): 887−891.

[3] INOUE A, ZHANG T. Stabilization of supercooled liquid and bulk glassy alloys in ferrous and non-ferrous systems [J]. J Non-Cryst Solids, 1999, 250−252(2): 552−559.

[4] INOUE A, TAKEUCHI A. Recent progress in bulk glassy, nanoquasicrystalline and nanocrystalline alloys [J]. Mater Sci Eng A, 2004, A375−377: 16−30.

[5] TELFORD M. The case for bulk metallic glass [J]. Mater Today, 2004, 7(3): 36−43.

[6] KÜNDIG A A, LEPORI D, PERRY A J, ROSSMANN S, BLATTER A, DOMMANN A, UGGOWITZER P J. Influence of low oxygen contents and alloy refinement on the glass forming ability of $Zr_{52.5}Cu_{17.9}Ni_{14.6}Al_{10}Ti_5$ [J]. Mater Trans JIM, 2002, 43(12): 3206−3210.

[7] LIU C T, CHISHOLM M F, MILLER M K. Oxygen impurity and microalloying effect in a Zr-based bulk metallic glass alloy [J]. Intermetallics, 2002, 10(11/12): 1105−1112.

[8] YOKOYAMA Y, KOBAYASHI A, FUKAURA K, INOUE A. Oxygen embrittlement and effect of the addition of Ni element in a bulk amorphous Zr-Cu-Al alloy [J]. Mater Trans JIM, 2002, 43(3): 571−574.

[9] INOUE A, SHIBATA T, ZHANG T. Effect of additional elements on glass transition behavior and glass formation tendency of Zr-Al-Cu-Ni alloys [J]. Mater Trans JIM, 1995, 36(12): 1420−1426.

[10] YOKOYAMA Y, FKAURA K, INOUE A. Cast structure and mechanical properties of Zr-Cu-Ni-Al bulk glassy alloys [J]. Intermetallics, 2002, 10(11/12): 1113−1124.

[11] KISSINGER H E. Reaction kinetics in differential thermal analysis [J]. Analytical Chem, 1957, 29(11): 1702−1706.

[12] SHEN Jun, SUN Jian-fei, GAO Yu-lai, WANG Gang, XING Da-wei, CHEN De-min, ZHOU Bi-de. Crystallization of high stable $Zr_{55}Al_{10}Ni_5Cu_{30}$ bulk amorphous alloy [J]. Trans Nonferrous Met Soc China, 2003, 13(1): 59−63.

[13] GAO Y L, SHEN J, SUN J F, WANG G, XING D W, XIAN H Z, ZHOU B D. Crystallization behavior of ZrAlNiCu bulk metallic glass with wide supercooled liquid region [J]. Mater Lett, 2003, 57(13/14): 1894−1898.

[14] CHEN H S. A method for evaluating viscosities of metallic glasses from the rates of thermal transformations [J]. J Non-Cryst Solids, 1978, 27(2): 257−263.

[15] MURTY B S, HONO K. Nanoquasicrystallization of Zr-based metallic glasses [J]. Mater Sci Eng, 2001, A312(1−2): 253−261.

[16] GEBERT A, ECKERT J, SCHULTZ L. Effect of oxygen on phase formation and thermal stability of slowly cooled $Zr_{65}Al_{7.5}Cu_{17.5}Ni_{10}$ metallic glass [J]. Acta Mater, 1998, 46(15): 5475−5482.

[17] LIN X H, JOHNSON W L, RHIM W K. Effect of oxygen impurity on crystallization of an undercooled bulk glass forming Zr-Ti-Cu-Ni-Al alloy [J]. Mater Trans JIM, 1997, 38(5): 473−477.

[18] MURTY B S, PING D H, HONO K, et al. Influence of oxygen on the crystallization behavior of $Zr_{65}Cu_{27.5}Al_{7.5}$ and $Zr_{66.7}Cu_{33.3}$ metallic glasses [J]. Acta Mater, 2000, 48(15): 3985−3996.

[19] LEE J K, BAE D H, YI S, KIM W T, KIM D H. Effects of Sn addition on the glass forming ability and crystallization behavior in Ni-Zr-Ti-Si alloys [J]. J Non-Cryst Solids, 2004, 333(2): 212−220.

[20] CHEN M W, INOUE A, SAKURAI T, PING D H, HONO K. Impurity oxygen redistribution in a nanocrystallized $Zr_{65}Cr_{15}Al_{10}Pd_{10}$ metallic glass [J]. Appl Phys Lett, 1999, 74(6): 812−814.

[21] HNG H H, LI Y, NG S C, ONG C K. Critical cooling rates for glass formation in Zr-Al-Cu-Ni alloys [J]. J Non-Cryst Solids, 1996, 208(1−2): 127−138.

[22] KÜBLER A, ECKERT J, GEBERT A, SCHULTZ L. Influence of oxygen on the viscosity of Zr-Al-Cu-Ni metallic glasses in the undercooled liquid region [J]. J Appl Phys, 1998, 83(6): 3438−3440.

(Edited by LONG Huai-zhong)